Clinical Imaging 45 (2017) 1–7

Contents lists available at ScienceDirect

Clinical Imaging

journal homepage: http://www.clinicalimaging.org

Qualitative agreement and diagnostic performance of arterial spin labelling MRI and FDG PET-CT in suspected early-stage dementia Comparison of arterial spin labelling MRI and FDG PET-CT in suspected dementia

Kathleen Weyts [a,*], Meike Vernooij [a], Rebecca Steketee [a,b], Roelf Valkema [a], Marion Smits [a]

[a] Department of Radiology and Nuclear Medicine, Erasmus University Medical Center Rotterdam, 's-Gravendijkwal 230, 3015 CE Rotterdam, The Netherlands
[b] Alzheimercentrum Zuidwest Nederland, founded by the EMC ('s-Gravendijkwal 230, 3015 CE Rotterdam, NL) and Havenziekenhuis Rotterdam, Haringvliet 2, 3011 TD Rotterdam, The Netherlands

ARTICLE INFO

Article history:
Received 16 June 2016
Received in revised form 21 April 2017
Accepted 9 May 2017
Available online xxxx

Keywords:
ASL-MRI
Pseudo-continuous
FDG PET-CT
Dementia
Early stage

ABSTRACT

18FDG PET-CT is useful for early and differential diagnosis of dementia.
ASL-MRI seems an attractive alternative.
Visual agreement was calculated in 21 brain regions bilaterally in 9/11 patients with suspected early-stage dementia, excluding 2 patients due to ASL-MRI motion artefacts. Overall gross agreement was almost perfect and identical between and within modalities ($\kappa = 0.85–0.86$, $p < 0.05$).
Intermodality regional agreement was variable, moderate ($\kappa = 0{,}56$ in posterior cingulate) to perfect (including in precuneus), not different from intramodality agreement.
Diagnostic accuracy was 5/9 (56%) for ASL-MRI and 7/9 (78%) for FDG PETCT.
($p = 0.31$).
Clinical experience and optimisation may further improve ASL-MRI's performance.

1. Introduction

[^{18}F]fluoro-2-deoxy-D-glucose positron emission tomography computed tomography (FDG PET-CT) is the current functional and most frequently used imaging gold standard for early and differential diagnosis of neurodegenerative diseases [1]. Newer tracers, such as those for amyloid and tau pathology, are very promising in this respect, but not yet validated well enough in routine clinical practice to be considered as the gold standard in a group of unselected patients visiting the memory clinic. Arterial spin labelling magnetic resonance imaging (ASL-MRI) has been proposed as a non-invasive, practical alternative. It uses magnetically labelled blood water as an endogenous tracer [2,3] to evaluate cerebral blood flow (CBF). Given the tight coupling of cerebral glucose metabolism and perfusion [4,5] both functional markers could provide similar information although discrepancies are known to occur [6,7]. ASL-MRI is potentially as widely available as conventional MRI, fast and cheap as a short additional sequence to the routine MRI in dementia work-up. It has been shown fairly reliable for CBF measurement in healthy young and older volunteers [8,9] and finding quite consistent abnormalities in preclinical Alzheimer disease (AD) and APOε4 carriers [10–12], MCI, converters to AD [8,10,11,13–16] and (early) AD patients [8,11,13,15–20]. In AD typical perfusion defects have been described similar to those seen on FDG PET-CT [13,15–17,19,20]. Regional hyperperfusion occurs too, particularly in early AD, mostly medial temporal (and hippocampal) and (less) in the anterior cingulate and frontal cortex, striatum and globus pallidus, due to compensatory mechanisms, vasodilatation or inflammation [12,13,15,19,21]. Less is known about other dementia types like frontotemporal dementia (FTD) [20–23], Lewy body dementia (LBD) [22] or vascular dementia [24,25].The vast majority of these studies are performed at group level using voxelwise or other (semi)quantitative techniques, yet not available for clinical routine.

There are relatively few studies that directly compare FDG PET(-CT) and ASL-MRI. 2 in healthy subjects [26,27] and one in neurologically asymptomatic oncological patients [28] showed overall good correlation but with substantial regional variability [27]. Scarce, mostly (semi)-quantitative and less visual comparative studies in dementia showed also a fairly good correlation [29–34]. Only one study performed a visual analysis of both modalities [30], showing similar regional abnormalities and diagnostic accuracy in a small population of mild to moderate AD. Data on direct comparison of the two modalities in the early and preclinical stages [32,33], other dementia types [31,32] and with qualitative approach [32] (only of ASL-MRI data) are scarce.

The purpose of this study was to assess qualitative agreement and diagnostic performance of ASL-MRI versus FDG PET-CT in an unselected

* Corresponding author.
E-mail addresses: m.vernooij@erasmusmc.nl (M. Vernooij), r.steketee@erasmusmc.nl (R. Steketee), r.valkema@erasmusmc.nl (R. Valkema), marion.smits@erasmusmc.nl (M. Smits).

http://dx.doi.org/10.1016/j.clinimag.2017.05.008
0899-7071/

patient population with suspected early-stage, various type dementia or MCI, using a clinically relevant standardized visual scoring system.

2. Material and methods

2.1. Study population

All patients from the memory clinic newly imaged at our centre with both ASL-MRI and FDG PET-CT between January 2011 and August 2012 were retrospectively included. The number of new patients visiting our memory clinic is roughly 5–10 per week. The majority of these patients however are referred from elsewhere, with imaging (MRI and/or PET) performed elsewhere and not repeated at our centre. From those patients that do undergo imaging in our centre, only a small proportion underwent both MRI and PET imaging. A selection bias due to this imaging referral procedure cannot be excluded.

The included patients were all suspected of early/mild dementia or MCI without a clear clinical diagnosis after repeated neuropsychological and neurological investigations. Patients had had symptoms for at least 8 to 40 months, except for one very slowly progressor with symptoms since 9 years. Patients were excluded from our study if the interval between ASL-MRI and FDG PET-CT exceeded 26 weeks, clinical status had changed in between and if alcohol or substance abuse was present. Ethics committee gave approval for the study.

Best available diagnostic gold standard was the probable diagnosis made by the multidisciplinary dementia team based on all neuropsychological and medical findings, further established upon follow-up (of up to 4.5 years) and treatment response where applicable. The patient population was heterogeneous, with different dementia diagnoses, reflecting the reality of a memory clinic and patients referred for FDG-PET.

2.2. FDG PET-CT imaging protocol

Patients fasted ≥6 h, with blood glucose levels adequate (<7 mmol/l, mean 5,6 ± 0,5 mmol/l) before intravenous injection of a standard activity of 218 ± 12.7 megabecquerel (MBq) FDG. Patients rested in a quiet, warm room with eyes covered, and ears plugged. Scanning was performed 60 ± 5.0 min post-injection on a Biograph PET/CT (Siemens, Erlangen, DE, 128 or 40 slice CT), with low dose CT for attenuation correction and localisation, and PET acquisition of 10 min afterwards. For PET ultrahigh definition reconstruction (time of flight and true X) was used, with 5 iterations and 21 subsets, image matrix size of 512, zoom 2,0 and Gaussian filter at full width half maximum (FWHM) of 1.0 mm.

2.3. ASL-MRI imaging protocol

MR imaging was performed at 3 T (MR750 Discovery, GE Healthcare, Milwaukee, WI) using an 8 channel head coil for reception of signal. ASL was performed in addition to the routine dementia protocol, including high-resolution T1 weighted, T2 and T2* weighted, Fluid Attenuated Inversion Recovery (FLAIR) T2 weighted, and diffusion weighted imaging. ASL images were acquired using a pseudo-continuous labelling sequence (pCASL) with an interleaved 3D fast spin echo (FSE) stack of spiral readouts using 512 sampling points on 8 spirals, resulting in an isotropic voxel size of 3.3 mm^3 in a 24 cm field of view (FOV). Further imaging parameters included: echo time = 4.7 ms; repetition time = 6000 ms; post-labelling delay = 1525 ms; 3 NEX; total scanning time = 4:29 min. Ears were plugged and eyes not covered. CBF maps were calculated using the single-compartment model [35] implemented by the scanner manufacturer.

2.4. Image analysis

A standardized visual scoring system of perfusion and metabolic abnormalities was used, first evaluated in 3 test patients.

Rating of 18 supratentorial brain regions bilaterally with a summary of 3 cortical lobes (see Table 1) was done as 0 = normal, 1 = equivocal, and 2 = abnormally low (3-pointsystem). There was no score for hyperperfusion or -metabolism. Presence of asymmetry with most affected side was noted. To assess disagreement in a clinically and statistically meaningful analysis, only a difference by 2 points was considered as disagreement (i.e. normal versus abnormal was considered as disagreement, but equivocal versus normal or equivocal versus abnormal were not; note that this does not affect the assessment of accuracy, as this was based on final diagnosis).

For the asymmetry scores only left versus right hemispheric abnormality was considered as disagreement.

A forced probable diagnosis, which could be any kind of dementia or brain disease needed to be given. Diagnostic accuracy was determined as the number of cases of the correct diagnosis (AD, FTD, CBD as specified in Table 2) out of the total number of cases.

Images were assessed blinded for clinical information (except for age and sex), individually by 2 neuro-radiologists for ASL-MRI and 2 nuclear medicine physicians for FDG PET-CT, followed by a modality consensus reading.. Knowledge in the field was judged sufficient for a proper reading for all readers: both readers of ASL-MRI had at least 20 exams' experience. Experience was somewhat higher for FDG PET-CT readers: at least 50 exams' experience per reader as well as >200 exams with ^{99m}Tc-HMPAO.

Readers of ASL-MRI were not allowed to view FDG PET-CT images and vice versa. Use of low dose CT for FDG PET readers and only structural MRI for all readers was not prohibited, essentially to correlate anatomical regions, consistent with clinical practice. For the same reason, analysis was done without partial volume correction, believed not to have major impact on (visual) metabolic assessment [36–38].

2.5. Statistics

Inter- and intramodality agreement was assessed by Cohen's kappas calculation (+ 95% confidence intervals (CI)), for all patients and regions together, excluding summarizing lobar ratings being redundant information (global agreement).

Regional agreement was calculated for each region and lobe. Asymmetry agreement was assessed separately. Modality consensus readings served for intermodality agreement calculation. 2 kappas were not statistically different if their difference (+ 95% CI) contained 0, with

$$\sigma_{\text{difference}} = \sqrt{\sigma_1{}^2 + \sigma_2{}^{2.}}$$

Modality diagnostic accuracy after consensus readings and of each individual reader were assessed, statistically compared with Fisher exact Test, one-tailed ($p < 0.05$). Analyses were performed in StatSoft, Inc. (2011) STATISTICA (data analysis software system), version 10. www.statsoft.com., in excel (version 14.0.0 (100825), Microsoft Office 2011 for Mac, and based on Dyadic Data Analysis for Cohen's kappa [39].

3. Results

3.1. Study population

Eleven patients (mean (±SD) age 59 years ± 8.5 years) with MCI (N = 1) or suspected of an early dementia syndrome (N = 10) were included. Two patients were not evaluable only on ASL-MRI due to motion artefacts. Patient characteristics and diagnoses of the 9 evaluable patients are listed in Table 2.

3.2. Intra- and intermodality agreement

3.2.1. Global agreement

Using 2-point scores (differentiating only clear disagreement between normal versus abnormal findings) inter- and intramodality

Table 1
Intra- and intermodality agreement.

		FDG PET-CT intramodality κ (95% CI)	ASL-MRI intramodality κ (95% CI)	ASL versus PET intermodality κ (95% CI)
Global supratentorial brain		0.85 (0.74–0.96)	0.86 (0.75–0.97)	0.85 (0.74–0.95)
Regional assessment				
Caudate nucleus		1.00 (0.54–1.00)	Non-calculable[a]	Non-calculable
Putamen		1.00 (0.54–1.00)	1.00 (0.54–1.00)	Non-calculable
Thalamus		Non-significant	1.00 (0.54–1.00)	Non-calculable
Frontal	Overall	1.00 (0.54–1.00)	0.48 (0.09–0.88)	0.67 (0.23–1.00)
	Inferior/Perisylvian	1.00 (0.54–1.00)	1.00 (0.54–1.00)	0.64 (0.21–1.00)
	Medial prefrontal	0.77 (0.32–1.00)	0.77 (0.32–1.00)	0.82 (0.37–1.00)
	Anterolateral prefrontal	1.00 (0.54–1.00)	1.00 (0.54–1.00)	0.67 (0.23–1.00)
Anterior cingulate		0.53 (0.12–0.93)	0.82 (0.37–1.00)	1.00 (0.54–1.00)
Primary sensorimotor		1.00 (0.54–1.00)	1.00 (0.54–1.00)	1.00 (0.54–1.00)
(Anterior) insula		0.82 (0.37–1.00)	Non-calculable	1.00 (0.54–1.00)
Temporal	Overall	0.78 (0.33–1.00)	0.64 (0.18–1.00)	0.61 (0.15–1.00)
	Anterior temporal	0.88 (0.42–1.00)	0.77 (0.32–1.00)	0.82 (0.37–1.00)
	Mesotemporal (hippocampal)	1.00 (0.54–1.00)	0.68 (0.25–1.00)	0.73 (0.28–1.00)
	Temporal perisylvian	0.61 (0.18–1.00)	Non-calculable	Non-calculable
	Wernicke's area	1.00 (0.54–1.00)*	0.40 (0.03–0.77)*	0.64 (0.21–1.00)
Parietal	Overall	1.00 (0.54–1.00)	0.78 (0.33–1.00)	1.00 (0.54–1.00)
	Lateral	1.00 (0.54–1.00)	1.00 (0.54–1.00)	1.00 (0.54–1.00)
	Medial (Precuneus)	0.77 (0.32–1.00)	0.87 (0.41–1.00)	1.00 (0.54–1.00)
Posterior cingulate		0.77 (0.32–1.00)	1.00 (0.54–1.00)	0.56 (0.10–1.00)
Occipital	Visual cortex	Non-calculable	0.77 (0.32–1.00)	Non-calculable
	Remainder occipital lobe	Non-significant	1.00 (0.54–1.00)	1.00 (0.54–1.00)

[a] Kappa non-calculable if all reviewers gave the same score (100% agreement rate without chance correction).
* Significantly different ($p < 0.05$).

agreements were almost perfect and not significantly different (Table 1): intermodality $\kappa = 0.85$ (95% CI 0.74–0.95); ASL-MRI $\kappa = 0.86$ (95% CI 0.75–0.97) and FDG PET-CT $\kappa = 0.85$ (95% CI 0.74–0.96).

Using 3-point scores however agreement was poor: intermodality $\kappa = 0.23$ (95% CI 0.15–0.32), ASL-MRI $\kappa = 0.37$ (95% CI 0.29–0.46) and FDG PET-CT $\kappa = 0.33$ (95% CI 0.25–0.42); $p > 0.05$.

Agreements in asymmetry ratings (2-point score) were poor to very poor: intermodality $\kappa = 0.01$ (95% CI 0.00–0.16), only significantly lower than ASL-MRI $\kappa = 0.32$ (95% CI 0.12–0.53); and not significant from FDG PET-CT $\kappa = 0.22$ (95% CI 0.03–0.41).

3.2.2. Regional agreement (Table 1)

This ranged from moderate to perfect both between and within modalities differentiating only normal from abnormal regional scorings.

Only in Wernicke's region was there lower agreement between ASL-MRI than FDG PET-CT reviewers, both not different from the intermodality value, and without significant agreement difference between and within modalities for the other regions. Regional asymmetry agreement was not statistically interpretable.

Lowest and moderate intermodality agreement was found in the posterior cingulate (PCC): $\kappa = 0.56$ (95% CI 0.10–1.00), followed by the temporal lobe: $\kappa = 0.61$ (95% CI 0.15–1.00) and others. Perfect gross intermodality agreement was found in several regions including precuneus.

3.3. Diagnostic accuracy

Diagnostic modality accuracy (Table 2) for ASL-MRI was 5/9 (56%) and for FDG PET-CT 7/9 (78%), ($p = 0.32$).

Both ASL-MRI readers reached 5/9 (56%), disagreeing in only one patient, wrongly diagnosed by both (CBD and normal instead of FTD). Individual diagnostic accuracy was respectively 5/9 (56%) and 6/9 (67%) for FDG PET-CT readers, with initial agreement in only 4 patients, but complementary for consensus diagnosis.

Two patients were wrongly diagnosed after consensus on ASL-MRI and FDG PET-CT.

The first one was interpreted by both as probably normal, but diagnosed initially with a clinically mild CBD or atypical FTD; after 2 years of follow-up, this diagnosis was revised and changed to progressive supranuclear palsy (PSP).

FDG PET-CT and ASL-MRI showed only discretely asymmetrical, slightly discordant defects frontotemporal and striatal.

The second patient was diagnosed with limbic encephalitis, after referral for suspected dementia (Fig. 1).

Table 2
Patient characteristics, modality and gold standard diagnosis.

	Age	Sex	MMSE	Δ (w)[a]	Diagnosis FDG PET-CT	ASL-MRI	Gold standard diagnosis	Symptoms(Y)[b]	Follow-up (Y)[c]
1	64	M	26	−2.0	AD	AD	AD	3.0	4.5
2	69	M	26	−26.0	AD	AD	AD	9.0	1.9
3	46	F	25	0.4	AD	Normal	Limbic encephalitis	0.75	2.0
4	64	F	27	1.0	Probably normal	Normal	PSP	3.5	4.6
5	69	F	28	4.0	FTD	AD	FTD	2.0	0.1
6	57	F	30	23.0	Normal	Normal	Normal	1.5	1.3
7	61	M	29	18.0	FTD	FTD	FTD	0.8	1.2
8	44	M	26	1.0	FTD	CBD	FTD–MND[d]	3.0	2.7
9	60	F	27	17.0	AD	AD	AD	3.5	2.7

[a] The interval in weeks between both exams: negative if FDG PET-CT performed first.
[b] The interval in years between onset of symptoms and first imaging.
[c] The duration of follow-up in years after first imaging, further establishing clinical diagnosis.
[d] Frontotemporal dementia with motor neuron disease.

A further 2 FTD patients were wrongly diagnosed only on ASL-MRI, classifying the first as AD because of pronounced parietal hyposignal (discordant with metabolism), and the second as CBD (Fig. 2).

In 5 patients there was diagnostic agreement of which 4 were abnormal (Fig. 3).

4. Discussion

In this small pilot study comparing ASL-MRI to FDG PET-CT in a clinical setting, we found fairly high gross agreement, between and within modalities although this varied by brain region. Subtle differences in interpretation between modalities however were not taken into account, for instance an equivocal score on one modality versus a normal or abnormal score on the other modality, since we only considered a discrepancy of normal versus abnormal scores as disagreement.

FDG PET-CT seemed to have better intramodality agreement only in Wernicke's region and a somewhat higher consensus diagnostic performance, although not statistically significant. Given the small sample size, statistics and mostly the lack of difference should be interpreted with care. A potential bias was also the high number of patients with confirmed diagnosis of early dementia.

Assessment of regional agreement is more meaningful in this respect and given the variability in pathology. It showed a range of moderate to perfect, again gross agreements intermodality not different from intramodality values. Intermodality agreement was lowest and just moderate for the posterior cingulate, being an important region in AD, however perfect in our 3 AD patients. This is possibly partly due to reviewers' experience, but intramodality agreement was strong to perfect for both modalities. Metabolism and perfusion in this region are physiologically higher than average cortex which needs to be taken into account for adequate evaluation [40,41].

Only in Wernicke's region was the moderate intramodality ASL-MRI agreement significantly lower than for FDG PET-CT, not different from intermodality agreement also being relatively lower. This is probably due to uncertainty of the readers and some watershed artefacts [31,42,43] in ASL-MRI.

There was (very) poor agreement in rating asymmetry of metabolism/perfusion, both between but also within modalities, without a clear explanation (sensitive scoring?) nor regional/disease pattern.

Regarding diagnostic performance: in 2 out of 9 patients the correct diagnosis was only made by FDG PET-CT, but inversely in none only by ASL-MRI. Two additional patients were not interpretable only on ASL-MRI due to motion artefacts. Motion is a frequent problem with ASL-MRI [44], asking for implementation of motion correction algorithms and faster scanning. Acoustic noise protection against the high-pitched noise from this sequence may help further. It may seem surprising that the readers rated some scans as normal, knowing that they were rating scans from patients and not from controls. Images were assessed blinded for clinical information (except for age and sex). Readers only knew that these patients were suspected of an early dementia syndrome or MCI. Not all MCI patients show perfusion/metabolic abnormalities, especially those that are non-converters. It is therefore not surprising that some scans were read as normal.

In one patient there was no diagnosis of dementia nor MCI upon follow-up. At the time of referral however, the patient was suffering from cognitive complaints since 8 months and suspected of a dementia

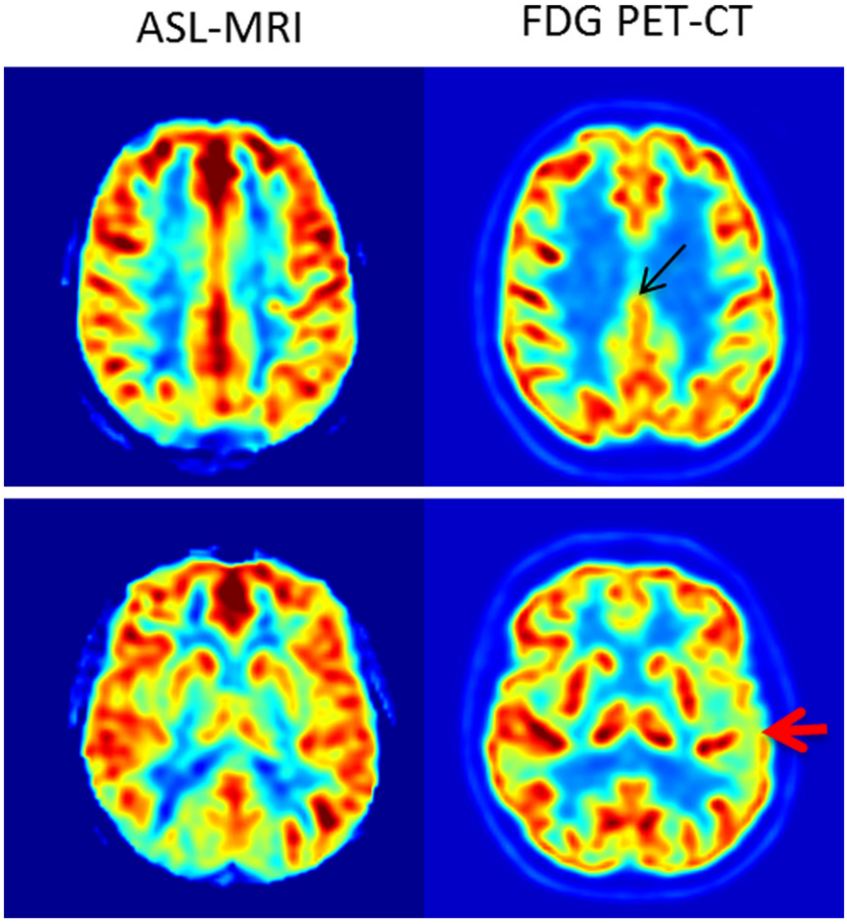

Fig. 1. Limbic encephalitis undiagnosed on both modalities 46-year-old female. On FDG PET-CT left parietotemporal (right, lower image, red arrow) and posterior cingulate hypometabolism (upper image, thin black arrow), classified as probable AD. Normal ASL-MRI. (For interpretation of the references to color in this figure legend, the reader is referred to the web version of this article.)

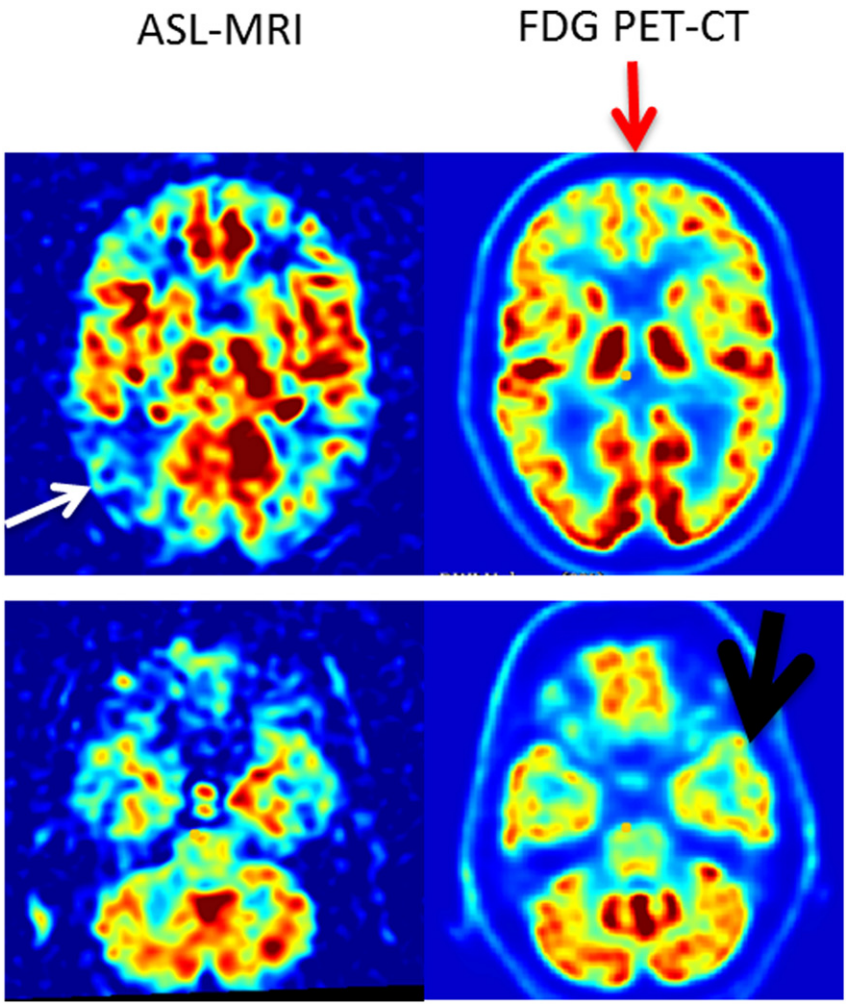

Fig. 2. FTD only diagnosed on FDG PET-CT 55-year-old male. On FDG PET-CT slight frontal (right, upper image, red arrow) and doubtful left temporal (lower right image, black thick arrow) hypometabolism. On ASL-MRI discrete asymmetry (right worse) and additional parietal hypoperfusion (left, upper image, white arrow), inducing a false diagnosis of CBD. (For interpretation of the references to color in this figure legend, the reader is referred to the web version of this article.)

syndrome. Upon follow-up, the diagnosis of limbic encephalitis was made. It would have been inappropriate to post-hoc exclude this patient as this would have introduced a selection bias.

Several potential reasons for the somewhat better diagnostic **p**erformance of FDG PET-CT in this patient group can be identified. First, ASL-MRI is sensitive to underestimating perfusion at the borderzone (watershed) areas of two vascular territories where a longer arterial transit time exists, becoming more pronounced with ageing when CBF decreases [30,42,43].

The lateral parietal watershed area is particularly problematic. Two FTD patients, incorrectly diagnosed only with ASL-MRI were due to probably falsely overestimated parietal hypoperfusion. This (moderate) discordancy between perfusion and metabolism was however not found in regional gross (2-point score), less sensitive agreement.

Newly emerging ASL-MRI implementations such as with velocity selective ASL and multiple post-labelling delays or inversion times allowing for ATT correction [45] and longer post-labelling delay time of 2000 ms [46] may overcome this watershedding problem.

Second, more extensive and complementary experience of our FDG PET-readers could have played a role especially in the diagnostic performance. ASL-MRI has only recently become available on clinical scanners, and, even though there is already an extensive body of research literature, clinical experience with ASL-MRI is still fairly limited.

Finally, cerebral perfusion is thought to be more (patho)physiologically variable than glucose metabolism, and the absolute perfusion measurement by H_2O^{15} PET has also been found to have a lower diagnostic power for AD than in FDG PET studies [47].

Two patients (22%) were incorrectly diagnosed with both modalities, both with rather rare diagnosis. Limbic encephalitis is a broad entity with variable possible FDG PET abnormalities [48]. No literature exists on the findings with ASL-MRI. The second patient was clinically diagnosed with probable mild CBD initially, and this diagnosis was revised after 2 years follow-up as PSP. Both FDG PET-CT and ASL-MRI showed only slight abnormalities, incorrectly interpreted as (probably) normal. PSP is known to give typically symmetrical hypometabolism in the prefrontal cortex and caudate nucleus, thalamus, and mesencephalon on FDG PET [49]. No literature has been found on findings of ASL-MRI in PSP.

The main limitation of this study is the small patient population. The limited power did not allow for correction for multiple comparisons, which does not affect our overall conclusion that there were no clear differences between modalities. The small differences that we found could however be false positive due to multiple comparisons, and therefore should be interpreted with care. Also, only patients were included who were referred for both MRI and FDG PET-CT, which is only a small proportion of our memory clinic's patient population. This will likely have introduced a selection bias towards those cases in whom clinical diagnosis is difficult.

However, several strengths highlight its value. Most importantly, in contrast to other studies comparing ASL-MRI with FDG PET-CT, ours is

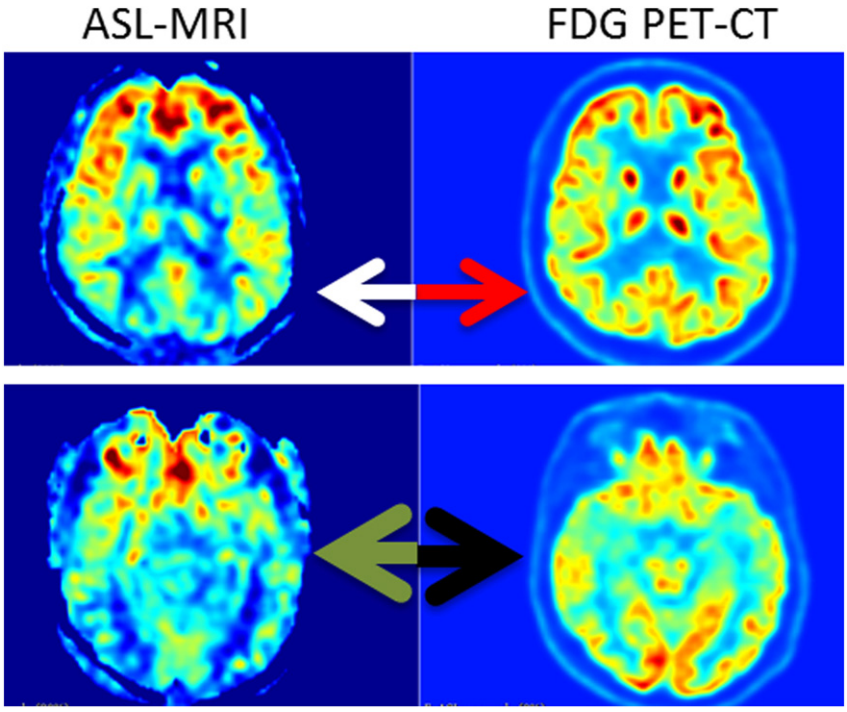

Fig. 3. AD diagnosed on both modalities 60-year-old female. Concordant bilateral hypometabolism and hypoperfusion, parietal (left: ASL-MRI upper image, white arrow, right: FDG PET-CT, upper image, red arrow) and temporal (left: ASL-MRI, lower image, green arrow, right: FDG PET-CT, lower image, black arrow). (For interpretation of the references to color in this figure legend, the reader is referred to the web version of this article.)

set in a true clinical context. Patients, although retrospectively included, were not selected based on their underlying disease process but represent a true reflection of patients referred for functional imaging in the context of diagnostic uncertainty in early-stage dementia syndrome. Also, our visual analysis reflects clinical routine evaluation, but is time consuming. It is not surprising that ours is only the second study [30], with findings in line with the previous exploratory study by Musiek et al., also reporting moderate to strong intermodality agreement, only in AD patients and healthy controls. They, however, found better intramodality agreement for FDG PET reads. However the two reviewers, reading both FDG PET and ASL-MRI scans, had more extensive experience with FDG PET.

We didn't perform quantification to resemble again clinical routine, nor partial volume correction for the same reason and the latter probably without major influence on (metabolic) evaluation [36–38]. One could consider the lack of co-registration of both modalities a further limitation, although all regions were well defined in advance.

5. Conclusions

ASL-MRI and FDG PET-CT showed overall good gross agreement both between and within modalities, and moderate to good diagnostic performance.

FDG PET-CT seemed to perform slightly better, partially related to readers' experience. Technical limitations, artefacts (mostly waters hedding) and (patho)physiological variability may further influence negatively ASL-MRI's diagnostic performance. Many of these technical issues are expected to be addressed in the near future, with more sophisticated ASL-MRI implementations and increasing expertise.

ASL-MRI could provide a good alternative to FDG PET-CT, if limited FDG PET-CT availability, in diabetics with difficult blood sugar control, and in the context of the rapidly increasing number of dementia patients. Our findings require confirmation in prospective, larger studies. Introduction of PET-MRI provides excellent opportunities for truly comparative modality studies under the same conditions.

Disclosure of funding sources

This research did not receive any specific grant from funding agencies in the public, commercial, or not-for-profit sectors.

Conflicts of interest

None

Acknowledgments

Figures in this article were created with the free platform software 3D Slicer:

Fedorov A, Beichel R, Kalpathy-Cramer J, Finet J, Fillion-Robin J-C, Pujol S, Bauer C, Jennings D, Fennessy F, Sonka M, Buatti J, Aylward S, Miller JV, Pieper S, Kikinis R (2012).

3D Slicer as an Image Computing Platform for the Quantitative Imaging Network. Magn Reson Imaging 30:1323-41. www.slicer.org.

References

[1] Landau SM, Harvey D, Madison CM, Reiman EM, Foster NL, Aisen PS, et al. Alzheimer's Disease Neuroimaging Initiative. Comparing predictors of conversion and decline in mild cognitive impairment. Neurology 2010;75:230–8.
[2] Detre JA, Leigh JS, Williams DS, Koretsky AP. Perfusion imaging. Magn Reson Med 1992;23:37–45.
[3] Williams DS, Detre JA, Leigh JS, Koretsky AP. Magnetic resonance imaging of perfusion using spin inversion of arterial water. Proc Natl Acad Sci U S A 1992;89:212–6.
[4] Jueptner M, Weiller C. Review: does measurement of regional cerebral blood flow reflect synaptic activity? Implications for PET and fMRI. NeuroImage 1995;2:148–56.
[5] Raichle ME. Behind the scenes of functional brain imaging: a historical and physiological perspective. Proc Natl Acad Sci U S A 1998;95:765–72.
[6] Vaishnavi SN, Vlassenko AG, Rundle MM, Snyder AZ, Mintun MA, Raichle ME. Regional aerobic glycolysis in the human brain. Proc Natl Acad Sci U S A 2010;107:17757–62.
[7] Vlassenko AG, Vaishnavi SN, Couture L, Sacco D, Shannon BJ, Mach RH, et al. Spatial correlation between brain aerobic glycolysis and amyloid-{beta} (A{beta}) deposition. Proc Natl Acad Sci U S A 2010;107:17763–7.
[8] Xu G, Rowley HA, Wu G, Alsop DC, Shankaranarayanan A, Dowling M, et al. Reliability and precision of pseudo-continuous arterial spin labeling perfusion MRI on 3.0 T

and comparison with 15O-water PET in elderly subjects at risk for Alzheimer's disease. NMR Biomed 2010;23:286–93.
[9] Zhang K, Herzog H, Mauler J, Filss C, Okell TW, Kops ER, et al. Comparison of cerebral blood flow acquired by simultaneous [15O] water positron emission tomography and arterial spin labeling magnetic resonance imaging. J Cereb Blood Flow Metab 2014;34:1373–80.
[10] Bangen KJ, Restom K, Liu TT, Wierenga CE, Jak AJ, Salmon DP, et al. Assessment of Alzheimer's disease risk with functional magnetic resonance imaging: an arterial spin labeling study. J Alzheimers Dis 2012;31:59–74.
[11] Kim SM, Kim MJ, Rhee HY, Ryu CW, Kim EJ, Petersen ET, et al. Regional cerebral perfusion in patients with Alzheimer's disease and mild cognitive impairment: effect of APOE epsilon4 allele. Neuroradiology 2013;55:25–34.
[12] Fleisher AS, Podraza KM, Bangen KJ, Taylor C, Sherzai A, Sidhar K, et al. Cerebral perfusion and oxygenation differences in Alzheimer's disease risk. Neurobiol Aging 2009;30:1737–48.
[13] Dai W, Lopez OL, Carmichael OT, Becker JT, Kuller LH, Gach HM. Mild cognitive impairment and Alzheimer disease: patterns of altered cerebral blood flow at MR imaging. Radiology 2009;250:856–66.
[14] Chao LL, Buckley ST, Kornak J, Schuff N, Madison C, Yaffe K, et al. ASL perfusion MRI predicts cognitive decline and conversion from MCI to dementia. Alzheimer Dis Assoc Disord 2010;24:19–27.
[15] Alexopoulos P, Sorg C, Forschler A, Grimmer T, Skokou M, Wohlschläger A, et al. Perfusion abnormalities in mild cognitive impairment and mild dementia in Alzheimer's disease measured by pulsed arterial spin labeling MRI. Eur Arch Psychiatry Clin Neurosci 2012;262:69–77.
[16] Binnewijzend MA, Kuijer JP, Benedictus MR, van der Flier WM, Wink AM, Wattjes MP, et al. Cerebral blood flow measured with 3D pseudocontinuous arterial spin-labeling MR imaging in Alzheimer disease and mild cognitive impairment: a marker for disease severity. Neuroradiology 2013;55:25–34.
[17] Alsop DC, Dai W, Grossman M, Detre JA. Arterial spin labeling blood flow MRI: its role in the early characterization of Alzheimer disease. J Alzheimers Dis 2010;20:871–80.
[18] Yoshiura T, Hiwatashi A, Yamashita K, Ohyagi Y, Monji A, Takayama Y, et al. Simultaneous measurement of arterial transit time, arterial blood volume, and cerebral blood flow using arterial spin-labeling in patients with Alzheimer disease. Am J Neuroradiol 2009;30:1388–93.
[19] Alsop DC, Casement M, de Bazelaire C, Fong T, Press DZ. Hippocampal hyperperfusion in Alzheimer's disease. NeuroImage 2008;42:1267–74.
[20] Steketee RM, Bron EE, Meijboom R, Houston GC, Klein S, Mutsaerts HJ, et al. Early-stage differentiation between presenile Alzheimer's disease and frontotemporal dementia using arterial spin labeling MRI. Eur Radiol 2016;26:244–53. http://dx.doi.org/10.1007/s00330-015-3789-x.
[21] Hu WT, Wang Z, Lee VM, Trojanowski JQ, Detre JA, Grossman M. Distinct cerebral perfusion patterns in FTLD and AD. Neurology 2010;75:881–8.
[22] Binnewijzend MA, Kuijer JP, van der Flier WM, Benedictus MR, Möller CM, Pijnenburg YA, et al. Distinct perfusion patterns in Alzheimer's disease, frontotemporal dementia and dementia with Lewy bodies. Eur Radiol 2014;24:2326–33.
[23] Du AT, Jahng GH, Hayasaka S, Kramer JH, Rosen HJ, Gorno-Tempini ML, et al. Hypoperfusion in frontotemporal dementia and Alzheimer disease by arterial spin labeling MRI. Neurology 2006;67:1215–20.
[24] Schuff N, Matsumoto S, Kmiecik J, Studholme C, Du A, Ezekiel F, et al. Cerebral blood flow in ischemic vascular dementia and Alzheimer's disease, measured by arterial spin-labeling magnetic resonance imaging. Alzheimers Dement 2009;5:454–62.
[25] Gao YZ, Zhang JJ, Liu H, Wu GY, Xiong L, Shu M. Regional cerebral blood flow and cerebrovascular reactivity in Alzheimer's disease and vascular dementia assessed by arterial spin labeling magnetic resonance imaging. Curr Neurovasc Res 2013;10:49–53.
[26] Newberg AB, Wang J, Rao H, Swanson RL, Wintering N, Karp JS, et al. Concurrent CBF and CMRGlc changes during human brain activation by combined fMRI-PET scanning. NeuroImage 2005;28:500–6.
[27] Cha YH, Jog MA, Kim YC, Chakrapani S, Kraman SM, Wang DJ. Regional correlation between resting state FDG PET and pCASL perfusion MRI. J Cereb Blood Flow Metab 2013;33:1909–14.
[28] Anazodo UC, Thiessen JD, Ssali T, Mandel J, Günther M, Butler J, et al. Feasibility of simultaneous whole-brain imaging on an integrated PET-MRI system using an enhanced 2-point Dixon attenuation correction method. Front Neurosci 2014;8:434.
[29] Chen Y, Wolk DA, Reddin JS, Korczykowski M, Martinez PM, Musiek ES, et al. Voxel-level comparison of arterial spin-labeled perfusion MRI and FDG-PET in Alzheimer disease. Neurology 2011;77:1977–85.
[30] Musiek ES, Chen Y, Korczykowski M, Saboury B, Martinez PM, Reddin JS, et al. Direct comparison of fluorodeoxyglucose positron emission tomography and arterial spin labeling magnetic resonance imaging in Alzheimer's disease. Alzheimers Dement 2012;8:51–9.
[31] Verfaillie SC, Adriaanse SM, Binnewijzend MA, Benedictus MR, Ossenkoppele R, Wattjes MP, et al. Cerebral perfusion and glucose metabolism in Alzheimer's disease and frontotemporal dementia: two sides of the same coin? Eur Radiol 2015;25:3050–9.
[32] Fällmar D, Lilja J, Velickaite V, Danfors T, Lubberink M, Ahlgren A, et al. Visual assessment of brain perfusion MRI scans in dementia: a pilot study. J Neuroimaging 2016;26:324–30.
[33] Tosun D, Schuff N, Jagust W, Weiner MW. Discriminative power of arterial spin labeling magnetic resonance imaging and 18F-fluorodeoxyglucose positron emission tomography changes for amyloid-β-Positive subjects in the Alzheimer's disease continuum. Neurodegener Dis 2016;16:87–94.
[34] Verclytte S, Lopes R, Lenfant P, Rollin A, Semah F, Leclerc X, et al. Cerebral hypoperfusion and hypometabolism detected by arterial spin labeling MRI and FDG-PET in early-onset Alzheimer's disease. J Neuroimaging 2016;26:207–12.
[35] Buxton RB, Frank LR, Wong EC, Siewert B, Warach S, Edelman RR. A general kinetic model for quantitative perfusion imaging with arterial spin labeling. Magn Reson Med 1998;40:383–96.
[36] Ibáñez V, Pietrini P, Alexander GE, Furey ML, Teichberg D, Rajapakse JC, et al. Regional glucose metabolic abnormalities are not the result of atrophy in Alzheimer's disease. Neurology 1998;50:1585–93.
[37] Shimizu S, Zhang Y, Laxamana J, Miller BL, Kramer JH, Weiner MW, et al. Concordance and discordance between brain perfusion and atrophy in frontotemporal dementia. Brain Imaging Behav 2010;4:46–54.
[38] Meltzer CC, Zubieta JK, Brandt J, Tune LE, Mayberg HS, Frost JJ. Regional hypometabolismin Alzheimer's disease as measured by positron emission tomography after correction for effects of partial volume averaging. Neurology 1996;47:454–61.
[39] Kenny DA, Kashy DA, Cook WL. Dyadic data analysis. Guilford Press; 2006(p 41).
[40] Silverman Daniel HS. PET in the evaluation of Alzheimer's disease and related disorders. New York: Springer; 2009(p.40).
[41] Pfefferbaum A, Chanraud S, Pitel AL, Shankaranarayanan A, Alsop DC, Rohlfing T, et al. Volumetric cerebral perfusion imaging in healthy adults: regional distribution, laterality, and repeatability of pulsed continuous arterial spin labeling (PCASL). Psychiatry Res 2010;182:266–73.
[42] Takahashi H, Ishii K, Hosokawa C, Hyodo T, Kashiwagi N, Matsuki M, et al. Clinical application of 3D arterial spin-labeled brain perfusion imaging for Alzheimer disease: comparison with brain perfusion SPECT. Am J Neuroradiol 2014;35:906–11.
[43] Zaharchuk G, Bammer R, Straka M, Shankaranarayan A, Alsop DC, Fischbein NJ, et al. Arterial spin-label imaging in patients with normal bolus perfusion-weighted MR imaging findings: pilot identification of the borderzone sign. Radiology 2009;252:797–807.
[44] Mutke MA, Madai VI, von Samson-Himmelstjerna FC, Zaro Weber O, Revankar GS, Martin SZ, et al. Clinical evaluation of an arterial-spin-labeling product sequence in steno-occlusive disease of the brain. PLoS One 2014;9:e87143.
[45] Zhang J. How far is arterial spin labeling MRI from a clinical reality? Insights from arterial spin labeling comparative studies in Alzheimer's disease and other neurological disorders. J Magn Reson Imaging 2016:1020–45.
[46] Alsop DC, Detre JA, Golay X, Günther M, Hendrikse J, Hernandez-Garcia L, et al. Recommended implementation of arterial spin-labeled perfusion MRI for clinical applications: a consensus of the ISMRM perfusion study group and the European consortium for ASL in dementia. Magn Reson Med 2005;73:102–16.
[47] Powers WJ, Perlmutter JS, Videen TO, Herscovitch P, Griffeth LK, Royal HD, et al. Blinded clinical evaluation of positron emission tomography for diagnosis of probable Alzheimer's disease. Neurology 1992;42:765–70.
[48] Heine J, Prüss H, Bartsch T, Ploner CJ, Paul F, Finke C. Imaging of autoimmune encephalitis—relevance for clinical practice and hippocampal function. Neuroscience 2015;309:68–83.
[49] Teune LK, Bartels AL, de Jong BM, Willemsen AT, Eshuis SA, de Vries JJ, et al. Typical cerebral metabolic patterns in neurodegenerative brain diseases. Mov Disord 2010;25:2395–404.